



# Alpha–Proton Differential Flow of the Young Solar Wind: Parker Solar Probe Observations

P. Mostafavi<sup>1</sup>, R. C. Allen<sup>1</sup>, M. D. McManus<sup>2</sup>, G. C. Ho<sup>1</sup>, N. E. Raouafi<sup>1</sup>, D. E. Larson<sup>2</sup>, J. C. Kasper<sup>3</sup>, and S. D. Bale<sup>2</sup>

<sup>1</sup> Johns Hopkins Applied Physics Laboratory, Laurel, MD 20723, USA; [parisa.mostafavi@jhuapl.edu](mailto:parisa.mostafavi@jhuapl.edu)

<sup>2</sup> Space Sciences Laboratory, University of California, Berkeley, CA 94720, USA

<sup>3</sup> Climate and Space Sciences and Engineering, University of Michigan, Ann Arbor, MI 48109, USA

Received 2021 November 5; revised 2022 January 18; accepted 2022 January 31; published 2022 February 24

## Abstract

The velocity of alpha particles relative to protons can vary depending on the solar wind type and distance from the Sun. Measurements from the previous spacecraft provided the alpha–proton differential velocities down to 0.3 au. The Parker Solar Probe (PSP) now enables insights into differential flows of the newly accelerated solar wind closer to the Sun for the first time. Here we study the difference between proton and alpha bulk velocities near PSP perihelia of encounters 3–7 when the core solar wind is in the field of view of the Solar Probe Analyzer for Ions instrument. As previously reported at larger heliospheric distances, the alpha–proton differential speed observed by PSP is greater for fast wind than the slow solar wind. We compare PSP observations with various spacecraft measurements and present the radial and temporal evolution of the alpha–proton differential speed. The differential flow decreases as the solar wind propagates from the Sun, consistent with previous observations. While Helios showed a small radial dependence of differential flow for the slow solar wind, PSP clearly showed this dependency for the young slow solar wind down to 0.09 au. Our analysis shows that the alpha–proton differential speed’s magnitude is mainly below the local Alfvén speed. Moreover, alpha particles usually move faster than protons close to the Sun. The PSP crossed the Alfvén surface during its eighth encounter and may cross it in future encounters, enabling us to investigate the differential flow very close to the solar wind acceleration source region for the first time.

*Unified Astronomy Thesaurus concepts:* [Solar wind \(1534\)](#); [Space plasmas \(1544\)](#); [Solar evolution \(1492\)](#); [Solar physics \(1476\)](#)

## 1. Introduction

The two primary ion components of the solar wind are protons and alpha particles (fully ionized helium), which have different properties from one another, such as density, velocity, and temperature (Marsch 2012; Verscharen et al. 2019). Alpha particles, which play an essential role in understanding the fundamental nature of the solar wind, have a much smaller number density compared to protons (Bame et al. 1997). Furthermore, their differential streaming with respect to protons was observed for the first time by Robbins et al. (1970). Since then, the alpha–proton differential velocity has been investigated by analyzing different spacecraft observations at various heliospheric locations. Even though alpha particles are heavier than protons, they tend to be faster than protons at distances close to the Sun (Feldman & Marsch 1997). Several works proposed different mechanisms for the superacceleration and heating of alphas, including drift instabilities (Verscharen et al. 2013b), resonant absorption of ion-cyclotron waves (Isenberg & Vasquez 2009; Kasper et al. 2013), and low-frequency Alfvén wave turbulence (Chandran 2010).

Previous spacecraft observations showed the dependence of the alpha–proton differential streaming on the solar wind speed (Marsch et al. 1982; Steinberg et al. 1996; Āurovcová et al. 2017). The slow solar wind, thought to be associated with the

streamer belt, typically comprises protons and alphas with comparable velocities. As the solar wind increases in speed up to that of the high-speed streams, likely originating from open magnetic fields associated with coronal holes, the alpha–proton differential streaming similarly increases. The dependence of the differential flow on the solar wind speed is more pronounced near the Sun and decreases with increasing heliodistance (see Figure 10 of Marsch et al. 1982). Thus, the dependence of the alpha–proton differential speed on the solar wind speed may indicate differences in solar wind acceleration between these different regions.

Various spacecraft at different heliographic distances enabled the study of the radial evolution of solar wind protons, alpha particles, and their differential velocities in the inner heliosphere from  $\sim 0.3$  to 5.5 au. Helios made observations from 0.3 to 1 au and showed that the average differential flow decreases with increasing heliocentric radial distance (Marsch et al. 1982; Āurovcová et al. 2019). Āurovcová et al. (2017) analyzed Wind observations at 1 au over 20 yr and, by comparing with Helios data, confirmed the differential velocity’s radial dependence. Furthermore, the alpha–proton differential speed at distances beyond Earth measured by Ulysses from 1 to 5.4 au was previously reported (Neugebauer et al. 1996; Reisenfeld et al. 2001). The observations showed that the differential speed continued to decrease with increasing distance until no significant differences were detected at large distances from the Sun ( $\sim 4$  au).

Additionally, observations of the solar wind by previous spacecraft show that the absolute value of the differential flow between alphas and protons usually stays lower than or

comparable to the local Alfvén speed (Marsch et al. 1982; Neugebauer et al. 1996; Berger et al. 2011; Āurovcova et al. 2017). The proposed explanation for the velocity limitation of the differential velocity is the wave–particle interaction driven by alpha–proton instabilities, which reduces the differential velocity down to the Alfvén speed (more details in Gary et al. 2000; Verscharen et al. 2013a). The alpha–proton differential velocity ( $V_{\alpha p}$ ) at about 0.3 au is often near this upper limit (i.e., the local Alfvén speed,  $V_A$ ; Marsch et al. 1982; Āurovcova et al. 2017). Neugebauer et al. (1996) showed that  $V_{\alpha p}/V_A$  decreases as the solar wind propagates and becomes close to zero at distances greater than  $\sim 4$  au, as observed by Ulysses. One of the suggested mechanisms that regulate the differential flow with increasing distance is Coulomb collisions (Kasper et al. 2008, 2017). Collisional age, which is the ratio of the time between alpha–proton Coulomb collisions and the transit time of the solar wind, increases with distance from the Sun and thus decreases the differential flow by leading the solar wind to thermodynamic equilibrium.

The present paper focuses on the alpha–proton differential flow of the young solar wind near the Sun (within 0.3 au) for the first time. In Section 2, we show the selection of the Parker Solar Probe (PSP) data. We statistically analyze PSP observations during close approaches of encounters 3–7 down to  $\sim 0.1$  au from the Sun to study this differential flow (Section 3). Moreover, we compare PSP measurements with observations from Helios, Wind, and Ulysses, spanning a wide range of heliospheric distances. This comparison shows the radial and temporal evolution of the proton and alpha and their relative speed. We compute the ratio between the alpha–proton differential speed and the local Alfvén speed of different solar wind types (i.e., slow, intermediate, and fast winds) to compare with previous studies. These results expand our knowledge about the solar wind’s origin and evolution from the Sun to larger distances. In Section 4, we summarize and conclude the paper.

## 2. Data Sources and Selection

Launched in 2018, PSP is a mission to study our Sun and young solar wind ions closer than any spacecraft before (Fox et al. 2016). The Solar Wind Electrons Alphas and Protons (SWEAP) on PSP consists of two ion sensors, the Solar Probe Cup (SPC) and the Solar Probe Analyzer for Ions (SPAN-I), that, combined, provide a continuous view of bulk solar wind ions (Kasper et al. 2016). The SPC is a Faraday cup that points directly to the Sun, while SPAN-I consists of a ram-facing electrostatic analyzer and time-of-flight section, which enables the differentiation of ions with distinct masses by sorting particles by their mass-per-charge ratio (more details in Livi et al. 2021). Due to the increasing spacecraft lateral velocity closer to the Sun, the solar wind ion flow in the spacecraft frame appears to move into the ram-facing side of PSP and, consequently, is within the field of view of SPAN-I. This paper, which uses the SPAN-I instrument to study alpha particles and their relative velocities to protons, focuses solely on intervals during the closest approaches of PSP when the tangential velocity of the spacecraft is sufficient to enable SPAN-I observations of the core of the particle distribution. Since the solar wind was largely not in the field of view of SPAN-I for the first two perihelia, we limit our statistical analysis to encounters 3–7 in this paper. While obtaining velocities from the partial moments (Livi et al. 2020a, 2020b) during times

when the core of the distribution is within the field of view of SPAN-I is generally robust, densities derived from these partial moments may still not be fully accurate, as the full ion distribution is not captured in the measurements. Therefore, we obtain the density from the analysis of the plasma quasi-thermal noise spectrum measured by the PSP/FIELDS Radio Frequency Spectrometer (more details in Moncuquet et al. 2020). During these perihelia, the PSP spacecraft had a perihelia of 0.166 au ( $35.67 R_s$ ) during encounter 3 and 0.095 au ( $20.35 R_s$ ) during encounter 7. We use the SPAN-I data product “sf0a” for the differential energy flux of alphas with the proton contamination subtracted, along with the “sf00” data product, which indicates the differential energy flux of the protons. The time resolutions of the SPAN-I proton and alpha particle observations are 7 and 14 s, respectively.

We also use magnetic field data from the FIELDS instrument (Bale et al. 2016, 2020) to compute the local Alfvén speed as

$$V_A = B / \sqrt{\mu_0(n_p m_p + n_\alpha m_\alpha)} = \tau B / \sqrt{\mu_0 n_e m_p}, \quad (1)$$

where  $B$  is the magnetic field,  $\mu_0$  is the permeability of vacuum,  $m_p$  and  $m_\alpha$  are the proton and alpha masses, and  $n_p$ ,  $n_\alpha$ , and  $n_e$  are the proton, alpha particle, and electron number densities, respectively. Due to the aforementioned uncertainty in the density computed from SPAN-I partial moments, we compute the Alfvén speed using  $n_e$ . Here  $\tau$  is a multiplicative factor proportional to the relative abundance of alpha particles in the solar wind. Using a range of alpha particle abundances from 2% to 6% of the solar wind,  $\tau$  ranges from 0.98 to 0.95, respectively. Thus, the Alfvén speeds reported in this paper (which assumes  $\tau = 1$ ) may overestimate the Alfvén speed by 2%–5%.

This paper focuses on statistical analysis of the differential velocity between protons and alpha particles. Some of the previous works analyzing alpha–proton differential velocity simply used the magnitude of the proton and alpha velocities to calculate their velocity differences  $|V_\alpha| - |V_p|$  (e.g., Neugebauer et al. 1994; Reisenfeld et al. 2001; Kasper et al. 2008). In this work, however, we calculate the differential speed based on  $|V_{\alpha p}| = |V_\alpha - V_p|$  to consider the directions of both vectors (e.g., similar to the work of Steinberg et al. 1996; Berger et al. 2011; Āurovcova et al. 2017). Furthermore, the cases with alpha particles faster than protons, and vice versa, are calculated using

$$V_{\alpha p} = \text{sign}(|V_\alpha| - |V_p|)|V_\alpha - V_p|. \quad (2)$$

## 3. Observations and Discussions

Figure 1 displays an example of the solar wind properties during a 2 hr interval from encounter 5. The top two panels show the azimuthal  $H^+$  and  $He^{++}$  fluxes (in the spacecraft frame) over time, illustrating the variation of the peak of the plasma distribution within the field of view of SPAN-I. In order to have reliable plasma moments for SPAN-I, we only investigate times when the core solar wind ions (proton and alpha) are primarily in the field of view of SPAN-I, typically only a couple of days during each encounter. The selection is done visually, as shown in Figure 1, which is a good example of the core distributions being within the field of view of SPAN-I (i.e., the peak in the flux-angle spectrogram in the top two panels is fully resolved and not along the top or bottom of the field of view). Proton and alpha speeds determined from

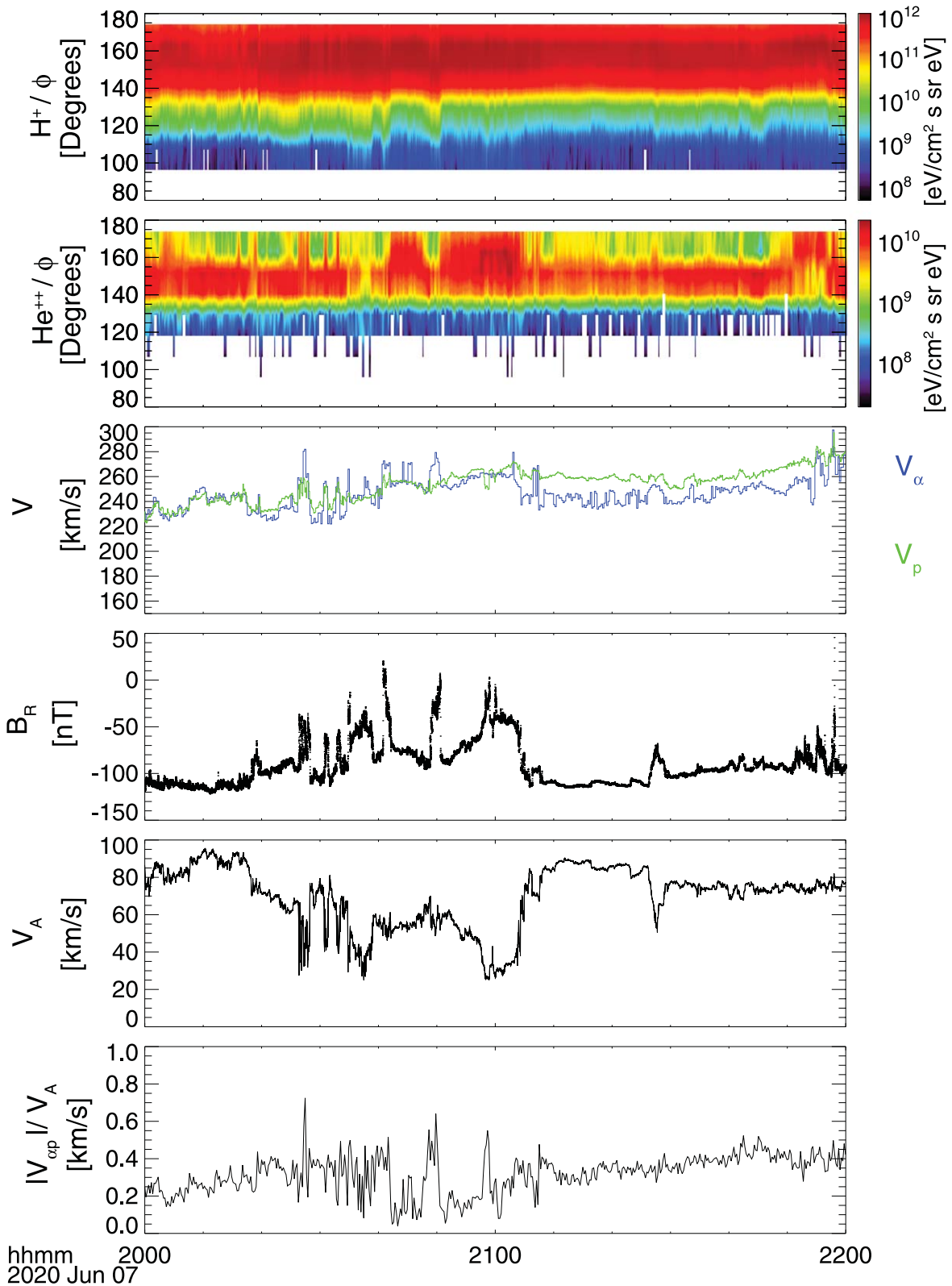


**Figure 1.** Solar wind properties over a 2 hr interval during encounter 5. From top to bottom are the  $\text{H}^+$  and  $\text{He}^{++}$  flux as a function of azimuthal angle ( $\phi$ ) in the spacecraft frame, proton and alpha velocities, radial component of the magnetic field, Alfvén speed, and magnitude of differential speed over local Alfvén speed.

moments are shown in the third panel of Figure 1. This particular period is comprised of a slow solar wind with the proton speed mostly exceeding that of the alpha particles. The bottom three panels show the radial magnetic field,  $B_R$ , the local Alfvén speed,  $V_A$ , and the differential velocity over

Alfvén speed,  $(|V_{\alpha p}|/V_A)$ . The alpha–proton differential speed is lower than the local Alfvén speed for such a slow solar wind, as previous missions observed at greater distances from the Sun (Marsch et al. 1982; Neugebauer et al. 1996). Previous studies have suggested that the Alfvén speed limits the alpha–proton

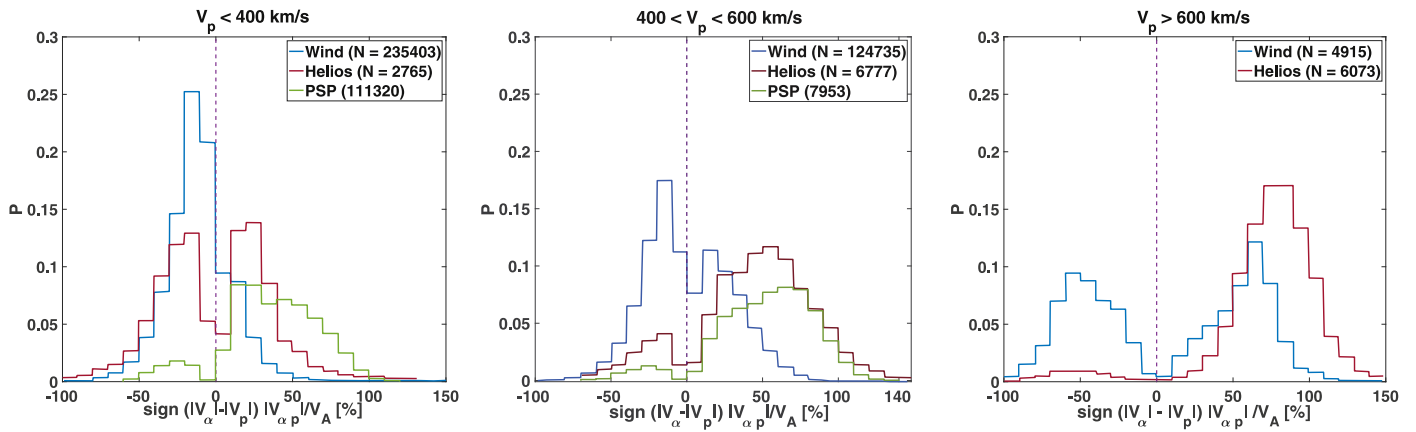


**Figure 2.** Probability distributions of the alpha–proton differential speed normalized to Alfvén speed for slow to fast solar wind speeds (from left to right). Wind data at 1 au (blue curves) and Helios data between 0.3 and 0.7 au (red curves) are adapted from Āurovcova et al. (2017) and Marsch et al. (1982), respectively. Green curves are PSP observations close to the Sun at about 0.1 au. Here  $N$  is the number of data sets used for each analysis.

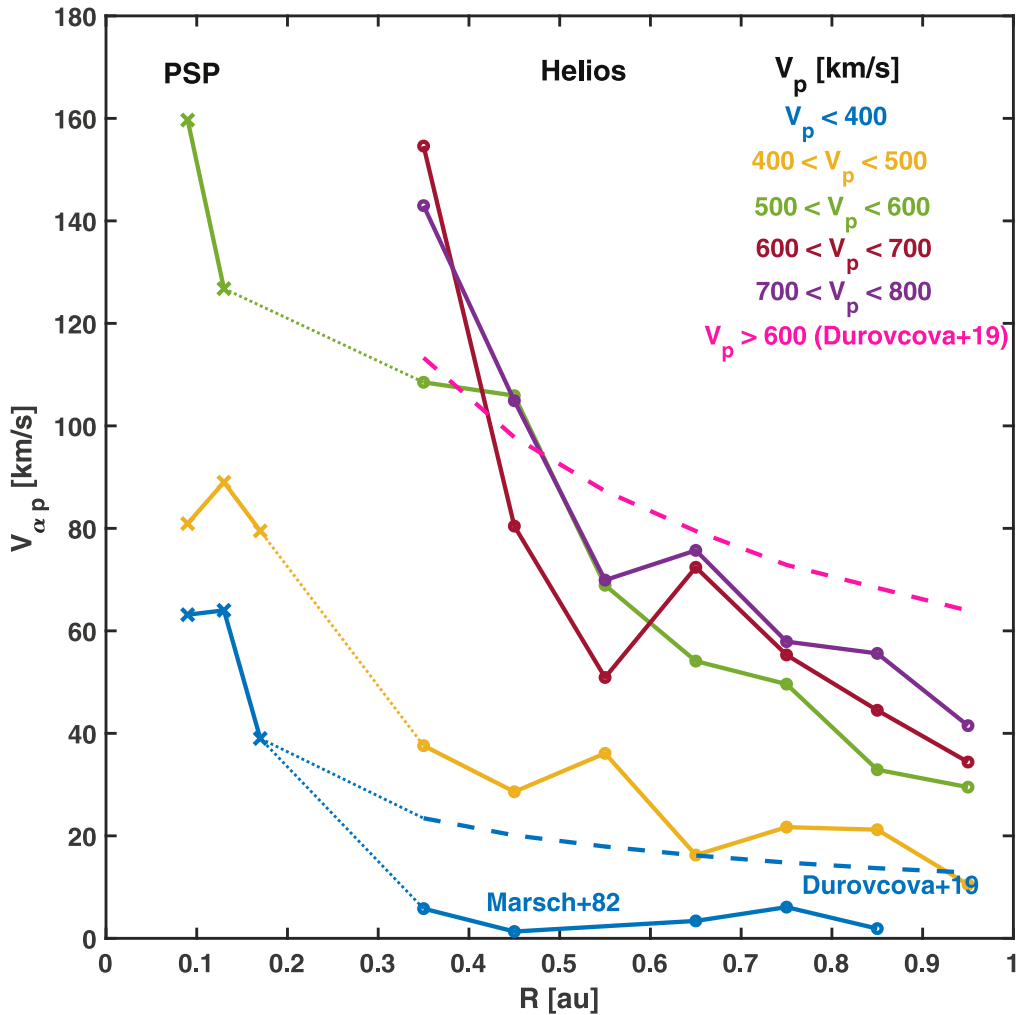
differential velocity due to wave–particle interactions driven by alpha–proton instabilities (Gary et al. 2000; Kasper et al. 2008). Once the alpha-to-proton drift exceeds  $V_A$ , it excites waves and instabilities in the plasma, such as the fast magnetosonic/whistler instability (Gary et al. 2000; Li & Habbal 2000) and the Alfvén/ion-cyclotron instability (Verscharen et al. 2013a). The generated waves interact with particles to satisfy the instabilities’ threshold and thus limit  $V_{\alpha p}$  by its upper bound (i.e.,  $V_{\alpha p} < V_A$ ).

Figure 2 compares young solar wind data at about 0.1 au from PSP (green curves) with Helios observations from 0.3 to 0.7 au (red curves from Marsch et al. 1982) and Wind measurements at 1 au (blue curves from Āurovcova et al. 2017). Each panel shows the probability distributions of the alpha–proton differential speed normalized to  $V_A$  for different solar wind types. In comparison with previous spacecraft data, we divided our data set into three different categories: slow- ( $V_p < 400 \text{ km s}^{-1}$ ), intermediate- ( $400 \text{ km s}^{-1} < V_p < 600 \text{ km s}^{-1}$ ), and high- ( $V_p > 600 \text{ km s}^{-1}$ ) speed solar winds. Note that negative values of the normalized alpha–proton differential speed correspond to protons that travel faster than alpha particles, and positive values mean that alpha particles are faster than protons. The left panel, representing the slow solar wind, shows a preferred positive  $V_{\alpha p}$  in PSP data. The Helios observations have two nearly identical positive and negative peaks. At larger distances, Wind observations at 1 au show only one peak with negative  $V_{\alpha p}$ . The prevalence of faster alphas compared to protons in the PSP observations close to the Sun confirms the superacceleration or preferential acceleration of the alphas in the solar corona (Ryan & Axford 1975; Marsch et al. 1982). The number of negative  $V_{\alpha p}$  observations increases as a function of distance from the Sun, as can be seen by comparing PSP to Helios and Wind observations. This pattern strongly supports the alphas’ deceleration over distance during solar wind expansion (Neugebauer et al. 1994; Maneva et al. 2015). The intermediate solar wind speed is shown in the middle panel. Wind observations still have a preferred negative  $V_{\alpha p}$ , while both PSP and Helios observations show approximately similar shapes with preferred positive peaks. The likely reason for not seeing a significant shift in PSP data to higher positive normalized differential velocities is that most of the immediate solar wind periods sampled are close to  $400 \text{ km s}^{-1}$  and only contain a few periods with solar winds with speeds greater than  $500 \text{ km s}^{-1}$ . The right panel shows the fast solar

wind observed by Wind and Helios; however, PSP did not observe the high-speed solar wind during the intervals of encounters 3–7 when the core of the solar wind was within the field of view of SPAN-I. As solar activity increases and PSP gets more connected to relatively large coronal holes, we expect to see a high-speed solar wind (likely being characterized by positive  $V_{\alpha p}$  and almost no negative values). In general, the comparison of PSP data with Helios and Wind shows an approximate evolution pattern of young solar wind close to the Sun to 1 au. Note that the data from three spacecraft (Wind, Helios, and PSP) are measured during different solar minima.

Furthermore, Figure 2 shows that the  $V_{\alpha p}/V_A$  ratio is generally less than 1 for different solar wind velocities at 1 au based on Wind observations. Besides, the Helios observations show that the flow difference between protons and alpha particles stays lower than or comparable to  $V_A$  for most solar wind speeds. With our data set, which includes up to encounter 7, PSP has not seen many intervals with differential speeds greater than  $V_A$ .

The dependence of the differential speed on both solar wind speed and distance from the Sun is apparent in Figure 3. Data points from 0.3 to 1 au are reproduced from Helios observations, in which circles and dashed lines are from Marsch et al. (1982) and Āurovcova et al. (2019), respectively. The crosses inside 0.2 au on the left side of Figure 3 are collected by PSP close to the Sun. Figure 3 shows that PSP has only observed solar wind in the first three slow solar wind categories during our data sets of encounters 3–7. Additionally, there was no observed solar wind with  $V_p$  between 500 and  $600 \text{ km s}^{-1}$  during perihelia 3, when PSP was located at  $35 R_s$ . Generally, this figure shows that as the solar wind becomes faster at a fixed distance from the Sun, its differential speed with alpha particles increases accordingly. The solar wind speed dependence of the differential speed is clearly seen from Helios data (Marsch et al. 1982; Āurovcova et al. 2019). Young solar wind observations made by PSP are consistent with this dependency. The dotted lines in Figure 3 connect the various data sets and roughly estimate the change in differential speed between  $\sim 0.15$  and  $0.3 \text{ au}$ . Generally, the radial dependence of the differential velocity is discernible from observations between  $\sim 0.1$  and  $1 \text{ au}$ , as  $V_{\alpha p}$  decreases as the solar wind propagates from the Sun to more considerable distances. One possible explanation is that since  $V_A$  decreases with increasing distance, instabilities continuously decelerate alpha particles (Gary et al.



**Figure 3.** Averages of the alpha–proton differential flow of the Helios and PSP data sets as a function of distance from the Sun for different ranges of solar wind speeds. Helios data are from 0.3 to 1 au. Circles and dashed lines are reproduced from Marsch et al. (1982) and Āurovcova et al. (2019) fits, respectively. The PSP data are shown with crosses, and the dotted lines connect the different data sets.

2000) and thus their differential speed. Another possible reason is Coulomb collisions, which are found to be an essential mechanism to bring all species closer to thermal equilibrium at great distances from the Sun (Marsch et al. 1982; Kasper et al. 2008). Marsch et al. (1982), who analyzed Helios data during the limited time of a solar minimum, observed an almost constant  $V_{\alpha p}$  for the slow solar wind with  $V_p < 400 \text{ km s}^{-1}$  and thus suggested no radial dependence of differential velocity for slow solar winds. In another work, Āurovcova et al. (2019) reanalyzed both Helios 1 and 2 data over an extended period during the whole solar cycle and showed a slight dependency of  $V_{\alpha p}$  on the radial distance for the slow solar wind. Observations with PSP report that the differential speed increases with decreasing heliocentric distance, even for a slow solar wind during a solar minimum. The significant radial dependence of  $V_{\alpha p}$  was not as evident from the Helios data, which were farther away, as the slow ions were greatly thermalized before reaching the orbit of Helios.

Kasper et al. (2017) reported that preferential heating of the heavy ions is predominately active within some boundary near the Sun. Later, Kasper & Klein (2019) proposed that the boundary was well correlated to the solar Alfven critical surface (i.e., at about 20–40  $R_s$ ). The PSP crossed the Alfven surface for the first time on 2021 April 28 during its eighth

encounter for about 5 hr (Kasper et al. 2021). It will likely cross the Alfven surface in future encounters as well and thus will be able to measure the solar wind in this unexplored region directly. Subsequent PSP encounters will be critical to understanding the solar wind heating mechanism and the reason for preferential heating and acceleration of the alpha particles. Based on the Kasper & Klein (2019) observation and prediction,  $V_{\alpha p}$  should not increase significantly after crossing the Alfven point. However, if the superacceleration of alphas happens near the solar surface, then  $V_{\alpha p}$  should keep increasing during future PSP data observations.

To better investigate how the alpha–proton differential velocity changes as the solar wind propagates away from the Sun, Figure 4 shows  $V_{\alpha p}$  as a function of the time of arrival from the Sun to the point of observation by PSP, Helios, and Ulysses. Ulysses data are 6 hr averages of the differential speed during the first 5 yr of the mission (from 1991 to 1996) covering a large range of solar activities at heliographic latitudes from  $+80^\circ$  to  $-80^\circ$  and radial distances from 1.3 to 5.4 au (Neugebauer et al. 1996). Thus, the spread of observed  $V_{\alpha p}$  in the Ulysses data comes from the various solar wind velocities and sources. The time of arrival of the Helios data is computed from Marsch et al. (1982). The purpose of plotting various Helios data speeds with different colors is to

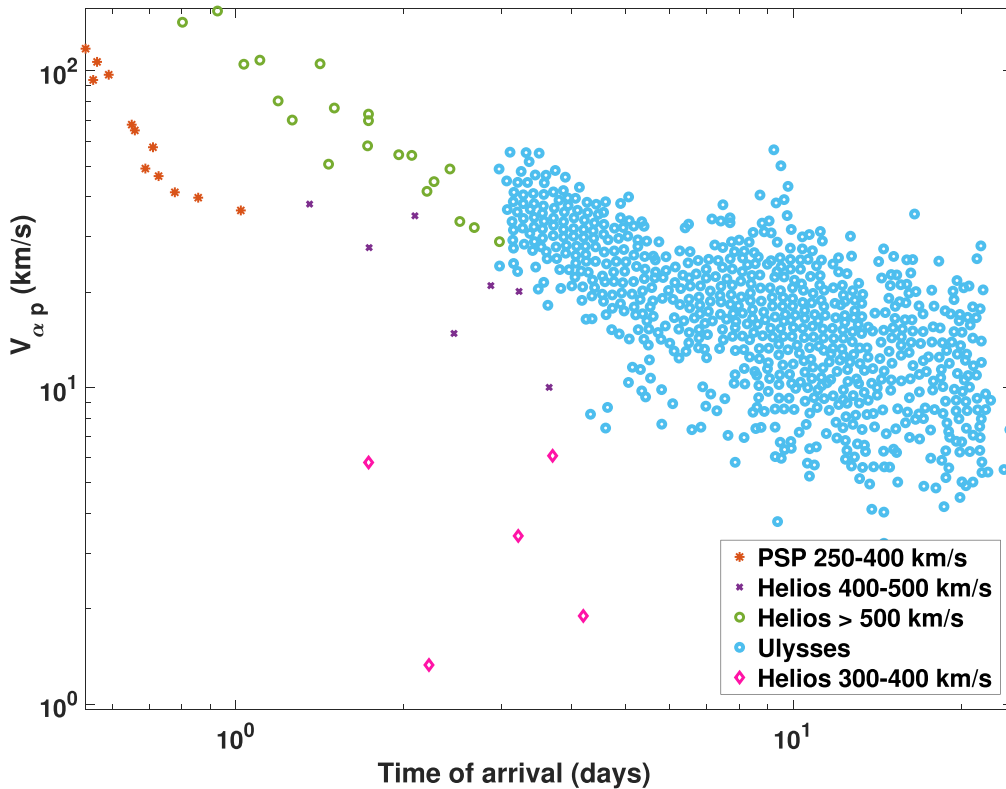


**Figure 4.** The 6 hr averages of the alpha–proton differential velocity are shown as a function of time of arrival to the spacecraft in a log–log scale. Helios and Ulysses data are adapted from Marsch et al. (1982) and Neugebauer et al. (1996), respectively.

distinguish different solar wind kinds. It is clearly obvious that a faster wind has a larger  $V_{\alpha p}$ , which may suggest that they have a different source than slow winds. The lowest speed of the Helios data with  $V_p = 300\text{--}400\text{ km s}^{-1}$  roughly follows a power law with the PSP data, whose 6 hr averages only include a solar wind with  $V_p = 250\text{--}400\text{ km s}^{-1}$ . Once again, this plot confirms the dependence of the differential flow on travel time and distance from the Sun. The slow solar wind observed by PSP has a significant differential flow with alpha particles, which decreases as it propagates into the heliosphere, reaching the orbit of Helios. As pointed out earlier, these observations are from different solar cycles, and the spacecraft do not measure the identical solar wind. The PSP mission encounters have thus far measured limited statistics, mainly characterized by a slow solar wind. Additional orbits of PSP, as we exit solar minimum with more available statistics, may provide faster solar wind speeds with more statistics to better compare with Helios observations.

#### 4. Conclusion

Our statistical analysis of PSP observations during encounters 3–7 confirmed that the alpha–proton differential velocity is positively correlated with the bulk solar wind speed. Thus, a differential flow between these two-particle populations may provide clues to the source of the solar winds and their acceleration and heating mechanism. We showed that the dependence of the differential flow on heliocentric distance continued inside 0.3 au, as observed by PSP. Furthermore, PSP clearly showed that this dependency is also valid for a slow solar wind, and they have larger alpha–proton differential speeds close to the Sun before their thermalizations ultimately occur. Close to the Sun, alpha particles are typically faster than

protons, showing their preferential acceleration mechanism. Our data set, which includes primarily slow solar wind, confirms that the magnitude of the alpha–proton differential speed is mainly below the local Alfvén speed. While the differential speed is oppositely correlated with the age of the solar wind, there is also a clear indication of a different speed of solar wind originating with various differential streaming. Whether this difference between fast and slow differential flows comes from distinct sources or some process, such as collisions as the solar wind advects outward, remains an open question. Forthcoming studies will aim to focus on the critical relationship between the Coulomb collisions or collisional age and proton–alpha differential speed. Moreover, we will analyze future PSP encounters at lower heliocentric distances, which may aid in our understanding of the superacceleration process of alpha particles close to the Sun. This will likely help answer the first science objective of PSP by explaining how the solar wind is heated and accelerated.

The Parker Solar Probe was designed and built and is now operated by the Johns Hopkins Applied Physics Laboratory as part of NASA’s Living with a Star (LWS) program (contract NNN06AA01C). Support from the LWS management and technical team has played a critical role in the success of the Parker Solar Probe mission. The authors would like to thank J. Verniero, R. Livi, and A. Rahmati for useful discussions. The authors acknowledge the Centre National d’Etudes Spatiales (CNES), the Centre National de la Recherche Scientifique (CNRS), the Observatoire de PARIS, NASA, and the FIELDS/RFS team for their support of the PSP/SQTN data production and the Centre de Données de la Physique des Plasmas (CDPP) for their archiving and provision. The FIELDS experiment on

the PSP spacecraft was designed and developed under NASA contract NNN06AA01C. Finally, we thank the reviewer for the constructive comments that helped to improve our paper.

### ORCID iDs

P. Mostafavi  <https://orcid.org/0000-0002-3808-3580>  
 R. C. Allen  <https://orcid.org/0000-0003-2079-5683>  
 M. D. McManus  <https://orcid.org/0000-0001-6077-4145>  
 G. C. Ho  <https://orcid.org/0000-0003-1093-2066>  
 N. E. Raouafi  <https://orcid.org/0000-0003-2409-3742>  
 D. E. Larson  <https://orcid.org/0000-0001-5030-6030>  
 J. C. Kasper  <https://orcid.org/0000-0002-7077-930X>  
 S. D. Bale  <https://orcid.org/0000-0002-1989-3596>

### References

- Bale, S. D., Goetz, K., Harvey, P. R., et al. 2016, *SSRv*, 204, 49
- Bale, S. D., MacDowal, R. J., Koval, A., et al. 2020, PSP FIELDS Fluxgate Magnetometer (MAG) Magnetic Field Vectors, Radial-Tangential-Normal, RTN, Coordinates, 4 samples/cycle, Level 2 (L2), 3.413 ms Data, doi:10.48322/wqcs-a534
- Bame, S. J., Asbridge, J. R., Feldman, W. C., & Gosling, J. T. 1997, *JGR*, 82, 1487
- Berger, L., Wimmer-Schweingruber, R. F., & Gloeckler, G. 2011, *PhRvL*, 106, 151103
- Chandran, B. D. G. 2010, *ApJ*, 720, 548
- Ďurovcová, T., Šafránková, J., Němeček, Z., & Richardson, J. D. 2017, *ApJ*, 850, 164
- Ďurovcová, T., Šafránková, J., & Němeček, Z. 2019, *SoPh*, 294, 7
- Feldman, W. C., & Marsch, E. 1997, in *Cosmic Winds and the Heliosphere*, ed. J. R. Jokipii, C. P. Sonett, & M. S. Giampapa (Tucson, AZ: Univ. Arizona Press), 617
- Fox, N. J., Velli, M. C., Bale, S. D., et al. 2016, *SSRv*, 204, 7
- Gary, S. P., Yin, L., Winske, D., & Reisenfeld, D. B. 2000, *GeoRL*, 27, 1355
- Isenberg, P. A., & Vasquez, B. J. 2009, *ApJ*, 696, 591
- Kasper, J. C., & Klein, K. G. 2019, *ApJL*, 877, L35
- Kasper, J. C., Lazarus, A. J., & Gary, S. P. 2008, *PhRvL*, 101, 261103
- Kasper, J. C., Maruca, B. A., Stevens, M. L., & Zaslavsky, A. 2013, *PhRvL*, 110, 091102
- Kasper, J. C., Abiad, R., Austin, G., et al. 2016, *SSRv*, 204, 131
- Kasper, J. C., Klein, K. G., Weber, T., et al. 2017, *ApJ*, 849, 126
- Kasper, J. C., Klein, K., Lichko, E., et al. 2021, *PhRvL*, 127, 255101
- Li, X., & Habbal, S. R. 2000, *JGR*, 105, 7483
- Livi, R., Larson, D. E., & Rahmati, A. 2020a, PSP Solar Wind Electrons Alphas and Protons (SWEAP) SPAN-A Proton Distribution Function, Partial Moments, Instrument Frame, Level 3 (L3), 7 s Data, doi:10.48322/ypyh-s325
- Livi, R., Larson, D. E., & Rahmati, A. 2020b, PSP Solar Wind Electrons Alphas and Protons (SWEAP) SPAN-A Alpha Particle Distribution Function, Partial Moments, Instrument Frame, Level 3 (L3), 14 s Data, doi:10.48322/ke19-2789
- Livi, R., Larson, D. E., Kasper, J. C., et al. 2021, Earth and Space Science Open Archive, doi:10.1002/essoar.10508651.1
- Maneva, Y. G., Ofman, L., & Vinās, A. 2015, *A&A*, 578, A85
- Marsch, E., Muhlauser, K. H., Rosenbauer, H., Schwenn, R., & Neubauer, F. M. 1982, *JGR*, 87, 35
- Marsch, E. 2012, *SSRv*, 172, 23
- Moncuquet, M., Meyer-Vernet, N., Issautier, K., et al. 2020, *ApJS*, 246, 2
- Neugebauer, M., Goldstein, B. E., Bame, S. J., & Feldman, W. C. 1994, *JGR*, 99, 2505
- Neugebauer, M., Goldstein, B. E., Smith, E. J., & Feldman, W. C. 1996, *JGRA*, 101, 17047
- Reisenfeld, D. B., Gary, S. P., Gosling, J. T., et al. 2001, *JGRA*, 106, 5693
- Robbins, D. E., Hundhausen, A. J., & Bame, S. J. 1970, *JGR*, 75, 1178
- Ryan, J. M., & Axford, W. I. 1975, *ZGeo*, 41, 221
- Steinberg, J. T., Lazarus, A. J., Ogilvie, K. W., Lepping, R., & Byrnes, J. 1996, *GeoRL*, 23, 1183
- Verscharen, D., Bourouaine, S., & Chandran, B. D. G. 2013a, *ApJ*, 773, 163
- Verscharen, D., Bourouaine, S., Chandran, B. D. G., & Maruca, B. A. 2013b, *ApJ*, 773, 8
- Verscharen, D., Klein, K. G., & Maruca, B. A. 2019, *LRSP*, 16, 1